Surface diffusion of hydrogen sulfide and sulfur dioxide in alumina membranes in the continuum regime

Sloot, H.J.; Swaaij, W.P.M. van; Versteeg, G.F.

Published in:
Journal of Membrane Science

DOI:
10.1016/0376-7388(92)80066-S

Publication date:
1992

Journal of Membrane Science, 74 (1992) 263-278
Elsevier Science Publishers B V , Amsterdam

Surface diffusion of hydrogen sulfide and sulfur dioxide in alumina membranes in the continuum regime

H.J. Sloot*, C.A. Smolders, W P M. van Swaaij and G.F. Versteeg
Twente University of Technology, Department of Chemical Engineering, P O Box 217, 7500 AE Enschede (The Netherlands)

(Received July 22, 1991, accepted in revised form July 21, 1992)

Abstract

Surface diffusion of H_2S and SO_2 in alumina membranes with an average pore diameter of ca 350 mm, impregnated with γ-Al_2O_3, is studied as a function of pressure at temperatures between 446 and 557 K Diffusion through the gas phase in the pores of the membrane almost entirely takes place in the continuum regime The pressure dependence of transport by diffusion through the gas phase and by surface diffusion is different, a fact which is used for the interpretation of the steady-state diffusion measurements It is observed that the contribution of surface diffusion to the total diffusion through the membrane can be as high as about 40% The surface diffusion data obtained are interpreted by a theoretical surface diffusion model using two parameters to be fitted, the product of the effective surface diffusion coefficient, the concentration of the adsorption sites and the adsorption parameter as well as the adsorption parameter itself The parameters fitted for SO_2 show a remarkable change between 498 and 525 K This probably maybe attributed to a change in the adsorbed species also reported in literature The parameters fitted for H_2S at different temperatures show a maximum, however, the product of the effective surface diffusion coefficient and the concentration of the adsorption sites increases with temperature

Keywords surface diffusion, alumina membranes, continuum regime, membrane reactor

1. Introduction

A novel type of membrane reactor has been developed in which the membrane is not used to separate components but to keep reactants separated from eachother [1] The reactants are fed to opposite sides of a porous membrane and diffuse into the membrane from either side. Therefore in principle no pressure difference is applied over the membrane contrary to the usual application of membranes The membrane contains a catalyst, or is catalytically active by itself, for a heterogeneously catalyzed chemical reaction between the reactants Provided that the rate of the reaction is fast compared to the diffusion rates of the reactants the process will be diffusion limited A reaction zone which is small compared to the membrane thickness will occur inside the membrane leading to a reaction plane in case of an instantaneous irreversible reaction. The location of the reaction zone inside the membrane will be such

Correspondence to G F Versteeg, Twente University of Technology, Department of Chemical Engineering, P O Box 217, 7500 AE Enschede, The Netherlands
*Present address Koninklijke/Shell Laboratorium, Amsterdam, P O Box 3303, 1003 AA Amsterdam, The Netherlands

that the molar fluxes of the reactants are in stoichiometric ratio. If the concentration of one of the reactants for some reason changes this will automatically result in a shift of the location of the reaction zone until the molar fluxes of both reactants are in stoichiometric ratio again. Finally the products will diffuse out of the membrane to both sides.

As a model reaction the Claus reaction [2] is used to study this membrane reactor

$$2\,H_2S + SO_2 \leftrightarrows \tfrac{3}{8}S_8 + 2\,H_2O \qquad (1)$$

The membrane used is made of α-Al_2O_3 with a mean pore diameter of ca. 350 nm impregnated with γ-Al_2O_3, a well known catalyst for the Claus reaction

The molar fluxes of the reactants into the membrane can be calculated assuming an instantaneous irreversible reaction inside the membrane and neglecting mass-transfer resistances in the gas phase outside the membrane. The transport is based on the combination of Knudsen and continuum diffusion through the gas phase in the pores of the membrane The calculation of the molar fluxes requires knowledge of the mean pore diameter and the porosity–tortuosity factor of the membrane. As a result of the assumptions the molar fluxes calculated are the highest possible provided that diffusion through the gas phase in the pores of the membrane is the only transport mechanism. Conversion measurements at a temperature of 549 K in the absence of a pressure difference over the membrane, however, resulted in effective diffusion coefficients of H_2S and SO_2 that seemed to be high compared to the continuum diffusion coefficients calculated from gas kinetic theory [1]. Possibly an additional transport mechanism takes place probably being surface diffusion. In order to verify the occurrence of surface diffusion of H_2S and SO_2 in the membrane, steady-state diffusion measurements, in the absence of a pressure difference over the membrane, were carried out that are discussed in the present study

2. Theory

Transport owing to the combination of diffusion through the gas phase in the pores of the membrane and surface diffusion is studied in the steady state using ceramic membranes with a flat sheet geometry. The total transport in the absence of a pressure difference over the membrane of component i owing to the combination of diffusion through the gas phase in the pores of the membrane and surface diffusion is described by eqn (2):

$$J_{i,\,\mathrm{tot}} = J_{i,\,\mathrm{gas}} + \frac{4}{d_p} J_{i,\,\mathrm{surf}} \qquad (2)$$

In the present study it was assumed that the pores could be regarded as ideally cylindrically shaped although this assumption is questionable for alumina membranes Another complicating factor is the homogeneity of the distribution of the γ-alumina over the α-alumina surface inside the membrane. As the main objective of the present study was to demonstrate the occurrence of surface diffusion effects in ceramic membrane reactors no special attention has been paid to the actual pore configuration Moreover, another pore shape only affects the value of the constants of the nominator of the term for $J_{i,\,\mathrm{surf}}$ in eqn. (2), e g rectangular pores have also a value of 4

The geometric factor $4/d_p$ in eqn (2) arises from the fact that transport owing to diffusion through the gas phase in the pores is proportional to the cross-sectional area of the pores, therefore proportional to d_p^2, whereas transport owing to surface diffusion is proportional to the circumference of the pores, therefore proportional to d_p The molar flux of component i through the gas phase in the pores of the membrane is described by Fick's law (eqn 3) using the Bosanquet formula for the combina-

tion of Knudsen and continuum diffusion by the principle of resistances in series.

$$J_{i,\,\mathrm{gas}} = -D^{\mathrm{eff}}_{i,\,\mathrm{gas}} \frac{P}{RT} \frac{\mathrm{d}x_i}{\mathrm{d}z} \tag{3}$$

with

$$\frac{1}{D^{\mathrm{eff}}_{i,\,\mathrm{gas}}} = \frac{1}{\frac{\epsilon}{\tau} D^{0}_{i,\,\mathrm{K}}} + \frac{1}{\frac{\epsilon}{\tau} D^{0}_{i,\,\mathrm{inert}}}$$

The Knudsen and continuum diffusion coefficients $D^{0}_{i,\,\mathrm{K}}$ and $D^{0}_{i,\,\mathrm{inert}}$ are calculated from the gas kinetic theory [3] The porosity–tortuosity factor ϵ/τ of the membrane is determined by permeation measurements with a pure gas

Surface diffusion is also described by Fick's law as presented by eqn (4)

$$J_{i,\,\mathrm{surf}} = -D^{\mathrm{eff}}_{i,\,\mathrm{surf}} c_{\mathrm{S}} \frac{\mathrm{d}\theta_i}{\mathrm{d}z} \tag{4}$$

In eqn. (4) c_{S} is the total concentration of adsorption sites on the surface (mole/m^2) and θ_i the fraction of the adsorption sites occupied by component i. Assuming that the adsorption and desorption kinetics are fast compared to the transport rates of component i through the pore and assuming a Langmuir adsorption isotherm, θ_i can be calculated by eqn. (5) in which b_i is the adsorption parameter.

$$\theta_i = \frac{b_i P x_i}{1 + b_i P x_i} \tag{5}$$

Substitution of eqn. (5) in eqn. (4) yields the expression for the molar flux owing to surface diffusion as a function of the driving force in the gas phase in the pores presented in eqn (6)

$$J_{i,\,\mathrm{surf}} = -D^{\mathrm{eff}}_{i,\,\mathrm{surf}} c_{\mathrm{S}} \frac{b_i P}{(1 + b_i P x_i)^2} \frac{\mathrm{d}x_i}{\mathrm{d}z} \tag{6}$$

From literature [4,5] it is known that the adsorption parameter b_i as well as the surface diffusion coefficient $D_{i,\,\mathrm{surf}}$ depends on the fraction of the adsorption sites occupied by component i, θ_i, owing to the fact that there usually is a distribution function of the heat of adsorption instead of a single value As the adsorption sites with a high heat of adsorption are occupied preferentially, an increase of θ_i results in a decrease of the average heat of adsorption of the remaining not-occupied adsorption sites This results in a decrease of the adsorption parameter b_i for these sites but at the same time in an increase of the mobility represented by $D_{i,\,\mathrm{surf}}$ for these sites. Therefore the product of $b_i D_{i,\,\mathrm{surf}}$ is expected to be relatively independent of the fraction of the adsorption sites occupied by component i, θ_i

Substitution of eqns. (3) and (6) in eqn. (2) results in the final expression for combined diffusion.

$$J_{i,\mathrm{tot}} = -\left(D^{\mathrm{eff}}_{i,\,\mathrm{gas}} \frac{P}{RT} + \frac{4}{d_{\mathrm{p}}} D^{\mathrm{eff}}_{i,\mathrm{surf}} b_i c_{\mathrm{S}} \frac{P}{(1 + b_i P x_i)^2} \right) \frac{\mathrm{d}x_i}{\mathrm{d}z} \tag{7}$$

Integration of eqn. (7) results in eqn. (8) which can be used for the interpretation of experimental data.

$$\frac{J_{i,\,\mathrm{tot}} L}{x_{i,\,\mathrm{int}\,0} - x_{i,\,\mathrm{int}\,L}} = D^{\mathrm{eff}}_{i,\,\mathrm{gas}} \frac{P}{RT} + \frac{4}{d_{\mathrm{p}}} D^{\mathrm{eff}}_{i,\,\mathrm{surf}} b_i c_{\mathrm{S}} \frac{P}{(1 + b_i P x_{i,\,\mathrm{int}\,0})(1 + b_i P x_{i,\,\mathrm{int}\,L})} \tag{8}$$

In eqn (8) $x_{i,\,\mathrm{int}\,0}$ and $x_{i,\,\mathrm{int}\,L}$ represent the molar fractions of component i at the membrane interface at $z=0$ and $z=L$ respectively. Mass transfer resistances in the gas phase outside the membrane, coupling the molar fractions at the membrane interfaces to the molar fractions in the bulk of the gas, are taken into account by eqns (9)

$$J_{i,\,\mathrm{tot}} = k_{\mathrm{g}} \frac{P}{RT} (x_{i,\,\mathrm{bulk}\,0} - x_{i,\,\mathrm{int}\,0}) \tag{9a}$$

$$J_{i,\,\mathrm{tot}} = k_g \frac{P}{RT}(x_{i,\,\mathrm{int}\,L} - x_{i,\,\mathrm{bulk}\,L}) \qquad (9b)$$

If the pore diameter of the membrane is sufficiently large and the pressure is sufficiently high, diffusion through the gas phase is taking place in the continuum regime The effective diffusion coefficient $D^{\mathrm{eff}}_{i,\,\mathrm{gas}}$ is therefore equal to the effective continuum diffusion coefficient which is inversely proportional to the pressure and so the first term in the right hand side of eqn (8) is independent of pressure. The second term in the right hand side of eqn. (8), representing transport owing to surface diffusion, however, is linearly dependent on the pressure, provided that the fraction of the adsorption sites covered by component i is relatively low. This difference in pressure dependence can be used to discriminate between both transport mechanisms

Rearrangement of eqn (8) results in eqn (10).

$$\frac{J_{i,\,\mathrm{tot}} L}{x_{i,\,\mathrm{int}\,0} - x_{i,\,\mathrm{int}\,L}} - D^{\mathrm{eff}}_{i,\,\mathrm{gas}} \frac{P}{RT} = \frac{\frac{4}{d_p} D^{\mathrm{eff}}_{i,\,\mathrm{surf}} b_i c_S}{(1 + b_i P x_{i,\,\mathrm{int}\,0})(1 + b_i P x_{i,\,\mathrm{int}\,L})} P \qquad (10)$$

The left hand side of eqn (10) is plotted as a function of pressure This should result in a straight line through the origin, the slope being equal to $(4/d_p) D_{i,\,\mathrm{surf}} b_i c_S$ provided that the fraction of the adsorption sites covered by component i is relatively low If the product in the denominator of eqn (10), $(1 + b_i P x_{i,\,\mathrm{int}\,0}) \times (1 + b_i P x_{i,\,\mathrm{int}\,L})$, is not close to unity this will result in a downward deviation of the straight surface-diffusion line at higher pressures

In porous media usually a distribution function of the pore diameter of the membrane is present It has to be determined whether this distribution has an influence on the overall molar fluxes that will be determined by experiments According to literature [6] the standard Johnson and Steward effective diffusion coefficient from steady-state diffusion measurements must be calculated from eqn. (11).

$$\bar{D}^{\mathrm{eff}}_i = \int_{d_p=0}^{d_p=\infty} D^{\mathrm{eff}}_i(d_p) \frac{\mathrm{d}f(d_p)}{\mathrm{d}d_p} \mathrm{d}d_p \qquad (11)$$

In eqn (11) $f(d_p)$ represents the volume fraction of pores with a diameter equal to d_p In the derivation of eqn (11), using the parallel pore model, it is assumed that the tortuosity of the pores is independent of the pore diameter Using the parallel pore model results in the maximal possible influence of the pore size distribution on the molar fluxes and this therefore can be regarded as a conservative approximation

The distribution function of the pore diameter of the impregnated membrane was measured using mercury porosimetry and is presented in Fig. 1.

As the determination of the distribution function of the pore diameter takes place with only a small part of the membrane as a sample, it was checked whether this distribution function is constant over the entire membrane. Therefore this measurement was also carried out with another sample of the same membrane The agreement of the average pore diameters calculated from both distribution functions was within 3% The average pore diameter of the membrane based on the pore area is 309 nm and based on the pore volume it is 322 nm, calculated by eqns. (12)

volume averaged

$$(\bar{d}_p)^2 = \int_{d_p=0}^{d_p=\infty} d_p^2 \frac{\mathrm{d}f(d_p)}{\mathrm{d}d_p} \mathrm{d}d_p \qquad (12a)$$

area averaged

$$\bar{d}_p = \int_{d_p=0}^{d_p=\infty} d_p \frac{\mathrm{d}f(d_p)}{\mathrm{d}d_p} \mathrm{d}d_p \qquad (12b)$$

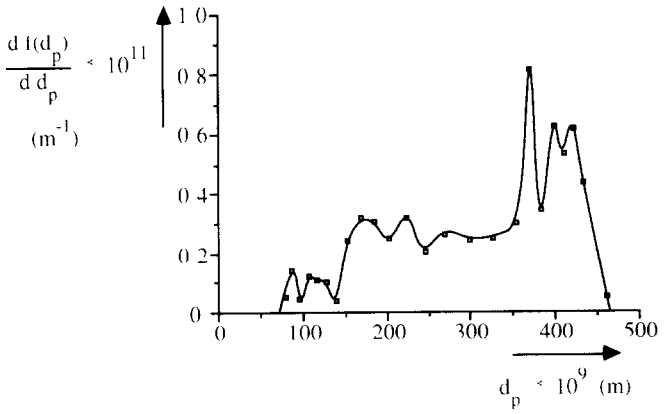

Fig 1 Distribution function of the pore diameter of the impregnated membrane

In the continuum regime in the presence of surface diffusion the overall effective diffusion coefficient as a function of the pore diameter can, according to eqn (7), be presented by eqn (13)

$$D_i^{\text{eff}}(d_p) = C_1 + \frac{C_2}{d_p} \tag{13}$$

Substitution of eqn (13) into eqn. (11) results in the expression that must be used to calculate the average pore diameter for the combination of continuum diffusion and surface diffusion

$$\frac{1}{\bar{d}_p} = \int_{d_p=0}^{d_p=\infty} \frac{1}{d_p} \frac{df(d_p)}{dd_p} dd_p \tag{14}$$

From eqn (14) an average pore diameter of 256 nm is calculated This average pore diameter has to be used in the factor $4/d_p$ in eqn. (10).

3. Experimental setup

The experimental setup used to measure molar fluxes through the membrane is presented schematically in Fig. 2.

Hydrogen sulfide in nitrogen or sulfur dioxide in nitrogen is fed by a mass flow controller to the membrane reactor to one side of the membrane and nitrogen is fed by a mass flow

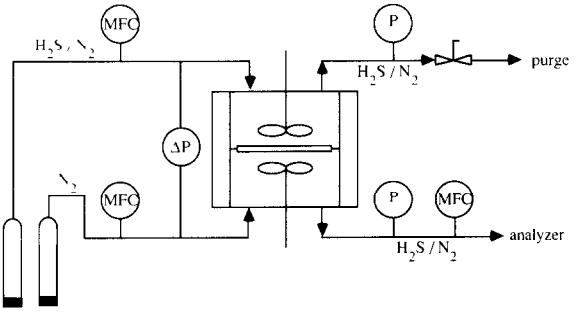

Fig 2 Experimental setup

controller to the other side of the membrane The reactor is made of stainless steel and consists of three parts, the upper chamber, a membrane holder and the lower chamber kept together by bolts. Both reactor chambers are well stirred and considered to be ideally mixed to simplify the interpretation The reactor is heated by an electric oven and the temperature in the reactor is controlled. The exit stream of the reactor at the nitrogen side of the membrane contains a mass flow controller This mass flow controller is used to keep the flow at the nitrogen side of the membrane constant which results in a pressure difference over the membrane of zero In order to check the pressure difference over the membrane a U-tube containing coloured water connects the two inlet streams just before the reactor The pres-

sure in the reactor is controlled by a flow regulator in the exit stream at the hydrogen sulfide in nitrogen side of the membrane The exit stream at the nitrogen side of the membrane containing hydrogen sulfide is analyzed by gas chromatography using a flame photometric detector The column used is a Chromosil column operated at a temperature of 323 K

In Fig 3 the sealing of the membrane in the stainless steel holder is presented schematically The membrane holder contains successively a sealing ring made of Fluorescent®, a mica reinforced teflon, the membrane, a second sealing ring, a pressure ring and a ring containing three bayonet catches by which it is connected to the stainless steel holder. This ring contains six 2 mm screws that, after tightening, are pressing on the pressure ring which is used to distribute the pressure exercised over the sealing ring The membrane holder is connected to the H_2S and SO_2 chambers by bolts on the outside For sealing between these compartments Fluorescent® rings are used again. The membranes used were obtained from ECN, Petten and were made of α-Al_2O_3 and had a flat sheet geometry with a diameter of 55 mm and a thickness of about 5 mm These membranes were impregnated with a saturated solution of

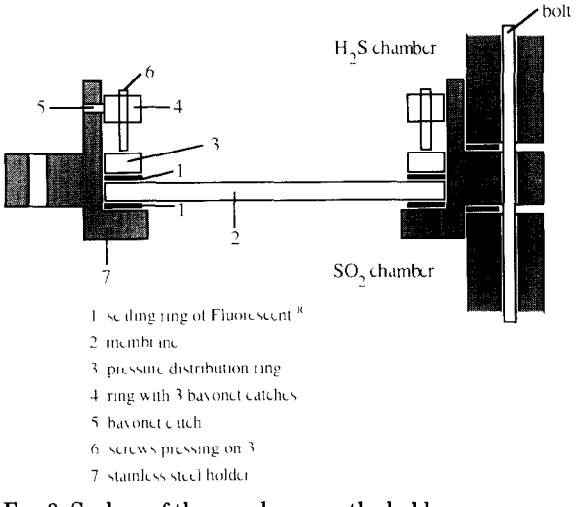

Fig 3 Sealing of the membrane in the holder

aluminum nitrate with ureum in water. After drying and calcining at 700 K for 2 hr γ-Al_2O_3 was obtained, the amount impregnated was of the order of 4 5 wt.%

Measurements were carried out in the steady state and the time required to obtain the steady state was of the order of 1 to 1.5 hr, the first measurement of each day requiring 3 to 4 hr to stabilize the system.

From the analysis the bulk concentration of hydrogen sulfide at the nitrogen side, which has diffused through the membrane, is determined and with the flow of nitrogen the molar flux of hydrogen sulfide times the membrane area is calculated The bulk concentration of hydrogen sulfide at the high concentration side of the membrane is calculated from an overall mass balance This balance was checked by analysing both exit streams together and the agreement was always within 0 5% As the molar flux of hydrogen sulfide times the membrane area was at least 20% of the flow of hydrogen sulfide into the reactor the accuracy of the molar flux of hydrogen sulfide or sulfur dioxide measured, based on the agreement of the overall mass balance, was always within 2 5%. The reproducibility of the measurements was always within a few percent

4. Determination of the porosity–tortuosity factor, ϵ/τ, of the membrane

In order to be able to subtract the molar flux through the gas phase in the pores of the membrane from the experimentally determined molar fluxes the porosity–tortuosity factor, ϵ/τ, of the membrane has to be determined The porosity–tortuosity factor of the membrane is measured by permeation measurements with a pure, non-adsorbing gas These permeation measurements consisted of forcing a pure gas through the membrane and measuring the pressure drop over the membrane as a function

of the flow through the membrane and the average pressure.

The transport through the membrane is in this case caused by the combination of Knudsen diffusion and viscous flow and is presented by eqn (15) (see e g., Ref [7]).

$$J_i = -\frac{1}{RT}\left(D_{i,K}^{eff} + \frac{B_0 P}{\eta}\right)\frac{dP}{dz} \qquad (15)$$

with

$$B_0 = \frac{\epsilon}{\tau}\frac{d_p^2}{32} \text{ and}$$

$$D_{i,K}^{eff} = \frac{\epsilon}{\tau}D_{i,K}^{0} = \frac{\epsilon}{\tau}\frac{d_p}{3}\sqrt{\frac{8RT}{\pi M_i}}$$

Integration of eqn (15) results in eqn. (16)

$$\frac{J_i}{\Delta P} = \frac{1}{RTL}\frac{\epsilon}{\tau}D_{i,K}^{0} + \frac{B_0}{RT\eta L}\bar{P} \qquad (16)$$

The average pressure in eqn. (16) follows directly from the integration and therefore it is not necessary to have a pressure drop over the membrane that is small compared to the pressure itself Plotting $J_i/\Delta P$ as a function of the average pressure should result in a straight line Both from the intercept and from the slope of this line the porosity–tortuosity factor of the membrane can be calculated. In order to check this experimental technique permeation measurements were performed both with nitrogen and with helium at a temperature of 533 K and using the impregnated membrane. In Fig 4 the results of nitrogen and helium are plotted according to eqn (16)

From the intercept and the slope of the lines in Fig 4 the effective Knudsen diffusion coefficient $D_{i,K}^{eff}$ and the membrane parameter B_0 are calculated respectively, both for helium and for nitrogen. Viscosity data required in the calculation were obtained from literature [8] In Table 1 the results for the parameters are given for helium and for nitrogen.

Before calculating the porosity tortuosity

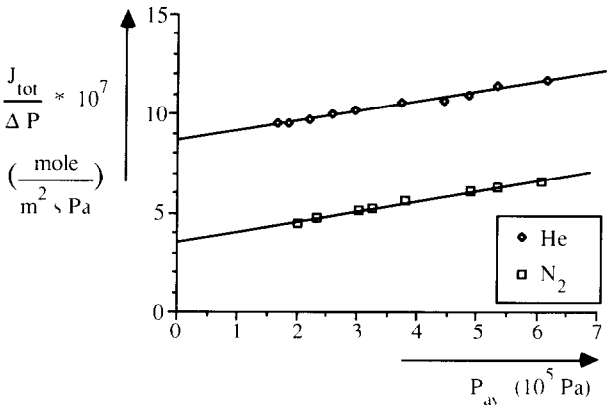

Fig 4 Permeation measurements with N_2 and He at a temperature of 533 K

TABLE 1

Parameters determined from the permeation measurements at 533 K

	He	N_2
$D_{i,K}^{eff}$ (m²/sec)	$1\,734\times10^{-5}$	$7\,011\times10^{-6}$
B_0 (m²)	$2\,87\times10^{-16}$	$2\,79\times10^{-16}$

factors from the data in Table 1 the results obtained for He are compared with those obtained for N_2 The values of B_0, being a membrane specific parameter, see eqn (15), determined with helium and nitrogen should be identical From Table 1 it can be concluded that the values agree within 3% The ratio of the effective Knudsen diffusion coefficients determined for helium and nitrogen should be equal to the inverse of the square root of the ratio of the molar masses of helium and nitrogen as can be seen from eqn (15) Comparing the experimentally determined ratio of the effective Knudsen diffusion coefficients of 2.473 with the theoretical ratio of 2 645 the agreement appears to be good as the deviation is about 6 5% Therefore from the results of the measurements with helium and nitrogen it can be concluded that this technique can be used to determine the characteristic membrane parameters.

From the effective Knudsen diffusion coefficient and from the value of B_0 the porosity–tortuosity factor of the membrane ϵ/τ can be calculated, see eqn. (15). As viscous flow is proportional to d_p^2 the average pore diameter to be used in the calculation of ϵ/τ from B_0 is the volume averaged pore diameter, 322 nm. However in the calculation of ϵ/τ from the effective Knudsen diffusion coefficient the area averaged pore diameter, 309 nm, must be used as Knudsen flow is proportional to d_p. The values of the porosity–tortuosity factor ϵ/τ calculated are given in Table 2.

From Table 2 it can be concluded that the porosity–tortuosity factor, ϵ/τ, of the membrane determined from the viscous flow parameter B_0 is about 24% lower compared to the value determined from the effective Knudsen diffusion coefficient A possible explanation is the use of the parallel pore model whereas in practice the distribution of the pore diameter can very well be located in the individual pores As the membrane parameter B_0 is proportional to d_p^2 whereas the effective Knudsen diffusion coefficient is proportional to d_p an obstruction inside the pore having a smaller pore diameter reduces viscous flow more effectively than Knudsen diffusion So the porosity–tortuosity factor, ϵ/τ, of the membrane calculated from B_0 is reduced more by the occurrence of an obstruction inside the pore compared to the porosity–tortuosity factor calculated from the effective Knudsen diffusion coefficient.

Because in the diffusion measurements transport is caused by diffusion processes and not by viscous flow, as there is no pressure difference over the membrane, the porosity–tortuosity factor ϵ/τ determined from the effective Knudsen diffusion coefficient will be used in the interpretation of the diffusion measurements

TABLE 2

Porosity–tortuosity factor ϵ/τ of the membrane

	He	N_2	average
$\frac{\epsilon}{\tau}$ (from $D_{i,K}^{eff}$)	0 092	0 099	0 096
$\frac{\epsilon}{\tau}$ (from B_0)	0 074	0 072	0 073

5. Determination of the mass transfer parameter in the gas phase, k_g

For the interpretation of diffusion data, the difference in the pressure dependence of diffusion through the gas phase in the pores of the membrane and surface diffusion is used. Therefore it is important to interpret the measured data using the correct pressure dependence of the mass transfer parameter in the gas phase, k_g, outside the membrane The mass transfer parameter, k_g, as a function of pressure and temperature can usually be described by a Sherwood (Re,Sc) relation as presented in eqn (17):

$$Sh = C_1 + C_2 Re^m Sc^n \tag{17}$$

with

$$Sh = \frac{k_g d}{D^0_{i,inert}}, \quad Re = \frac{\rho N d^2}{\eta} \text{ and } Sc = \frac{\eta}{\rho D^0_{i,inert}}$$

Values of m and n in eqn (17) as reported in literature, determined in gas–liquid systems in stirred cells with a smooth interface, are $m = 2/3$ and $n = 1/2$ [9]. For these gas–liquid systems it appeared that constant C_1 is negligible From eqn (17) and these values of m and n the dependency given in eqn (18) is calculated

$$k_g \sim (P)^{-1/3} (\eta T)^{-0\,17} (D^0_{i,inert})^{1/2} \tag{18}$$

with $D^0_{i,inert}$ the diffusion coefficient at a pressure of 10^5 Pa

Since the difference between the continuum diffusion coefficients at atmosferic pressure of H_2S and SO_2 in N_2 is about 30%, the k_g values for H_2S and SO_2 will differ only about 15%. The

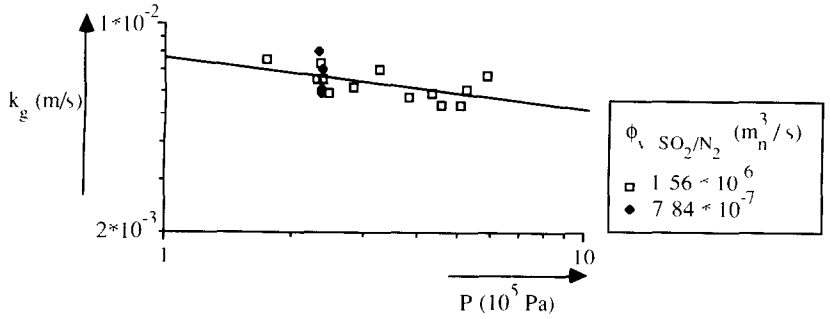

Fig 5 Mass transfer in the gas phase outside the membrane as a function of pressure

influence of the temperature on k_g in the range of 450 K to 550 K where diffusion measurements were performed, is limited to about 5%, according to eqn. (18). The difference of the k_g value between a pressure of 10^5 and 6×10^5 Pa, however, is about 50% according to eqn (18) Therefore, and to determine the value of the constant C_2 in eqn (17), k_g measurements were performed as a function of pressure in the experimental setup used for diffusion measurements

The mass transfer parameter in the gas phase outside the membrane, k_g, was measured by performing conversion measurements with H_2S and SO_2 at a temperature of 534 K. H_2S in N_2, with a H_2S molar fraction of 0 03, and SO_2 in N_2, with a molar fraction of SO_2 of 1500 ppm, are fed to opposite sides of the porous membrane Both reactants diffuse through the stagnant gas film outside the membrane into the membrane and react very fast resulting in a very small reaction zone as was pointed out in the introduction Owing to the high molar fraction of H_2S the location of this reaction zone is entirely shifted towards the membrane interface at the SO_2 side and mass-transfer limitation of SO_2 in the gas phase outside the membrane occurs In this situation slip of H_2S to the opposite side of the membrane occurs From the determination of the conversion of SO_2 the mass-transfer parameter k_g is calculated as a function of pressure To check whether the k_g values obtained are independent of the flow rate of the mixture of SO_2 and N_2, this flow rate was varied No influence on the k_g values calculated was observed In Fig 5 the mass transfer parameter k_g is given as a function of pressure. During these experiments the stirrer speed was kept constant at the same value as used in the diffusion measurements.

The mass transfer parameter k_g as a function of the pressure P can be described by eqn (19).

$$k_g = 7.53\times10^{-3}\times P^{-0\,16} \qquad (19)$$

with P in 10^5 Pa

Except for two data all experimentally determined k_g values can be described according to eqn. (19) within 15% Although in the present study k_g has been determined in a completely different experimental setup and conditions compared to those in Ref [9], the agreement between the pressure dependence of k_g determined, -0.16, and literature data [9], $-1/3$, can be regarded as remarkably. Especially if is taken into account that the interface of Versteeg et al. [9] was a freely moving gas–liquid interface and in the present study a fixed ceramic interface was used The k_g data given by eqn (19) are used in the interpretation of the diffusion measurements.

6. Results from diffusion measurements

Diffusion measurements as a function of pressure were performed both with H_2S and

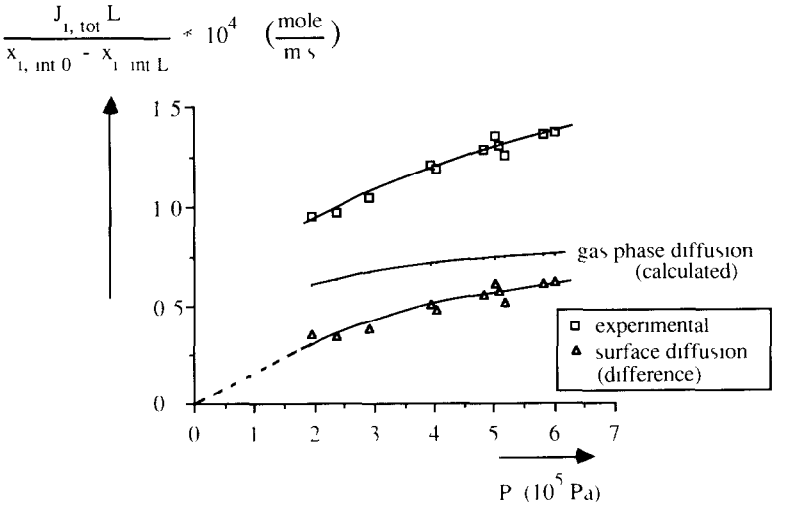

Fig 6 Diffusion data of SO_2 as a function of pressure at a temperature of 548 K

with SO_2 at temperatures between 450 K and 550 K. The interpretation of the diffusion data was performed according to eqn. (10). An example of the figures obtained is given in Fig 6 for SO_2 at a temperature of 548 K.

From Fig. 6 it can be seen that there is a substantial difference between the transport expected on the basis of only diffusion through the gas phase in the pores of the membrane and the experimentally observed transport; the difference amounts to 60 to 80% based on gas phase diffusion. From the fact that the line representing gas phase diffusion is not entirely independent of the pressure it can be concluded that the experiments performed at these lower pressures are not yet completely in the continuum regime Subtraction of the transport through the gas phase in the membrane from the experimentally determined transport gives the contribution of surface diffusion (see eqn. 10) The line representing surface diffusion, which according to eqn. (10) should pass through the origin, is not straight but curved Apparently the denominator in the surface diffusion term in eqn (10) plays a role, meaning that at the highest pressures the fraction of the adsorption sites covered by SO_2 is not negligibly small. As the curvature is caused by the adsorption parameter b_i the data can be used to determine both the product $D_{i,S}b_ic_S$ and b_i by a two-parameter fit of the experimental data Chosing values for the product $D_{i,S}b_ic_S$ and b_i, theoretical values of the surface diffusion contribution term of eqn (10), SDC_{theor}, can be calculated as a function of pressure from eqn (20) and compared with the experimental values, SDC_{exp}, presented by eqn (21)

$$SDC_{theor} = \frac{4}{d_p} D^{eff}_{i,S} b_i c_S \frac{P}{(1+b_i P x_{i,int\,0})(1+b_i P x_{i,int\,L})} \quad (20)$$

$$SDC_{exp} = \frac{J_{i,tot} L}{x_{i,int\,0} - x_{i,int\,L}} - D^{eff}_{i,gas} \frac{P}{RT} \quad (21)$$

The parameters $D_{i,S}b_ic_S$ and b_i are fitted minimizing the cumulative relative deviation function, CD, between the surface diffusion model and the experimental data by the expression given in eqn (22)

$$CD = \sum_{J=1}^{J=N} \left(\frac{SDC_{theor,J} - SDC_{exp,J}}{SDC_{av,J}} \right)^2 \quad (22)$$

with N the number of experimental data and

$$SDC_{av,j} = \frac{SDC_{theor,j} + SDC_{exp,j}}{2}$$

Successively now the data obtained for SO_2 and H_2S are discussed.

6 1 Surface diffusion data of SO_2 on γ-Al_2O_3

In Table 3 the fitted parameters for SO_2 are presented at different temperatures, also the calculated value of the product $D_{i,S}c_S$ and the average relative deviation between the theoretical surface diffusion model and the experimental data are given. A graphical comparison of the experimental surface diffusion data and the theoretically fitted data as a function of pressure at different temperatures is given in Fig 7

From Table 3 it can be seen that the parameters $D_{i,S}b_ic_S$ and b_i fitted can be divided into two groups, the data at temperatures of 447, 473 and 498 K and the data at 525 and 548 K The surface diffusion data within these two groups of temperatures are reasonably constant but there is a remarkable difference between the two groups of data From a change of the temperature of 498 to 525 K the fitted adsorption parameter, b_i, increases suddenly by about a factor of 10 whereas the value of the product $D_{i,S}b_ic_S$ increases by about a factor of 2. The values of the product $D_{i,S}c_S$ are only presented at the two highest temperatures as only in that situation an acceptable accuracy of the adsorption parameter b_i is present

Studies in literature concerning the adsorption of SO_2 on γ-Al_2O_3 reveal that there are different adsorbed species, physically adsorbed SO_2 and a weakly chemisorbed SO_2^- anion [10–13] Ono et al [11] studied the formation of SO_2^- anions on γ-Al_2O_3 as a function of temperature using electrospin resonance and found a maximum in the amount of SO_2^- anions at a temperature of 513 K of approximately 10 percent of the SO_2 adsorbed. Karge et al. [12] reported also a sudden decrease of the relative amount of SO_2^- anions, however, at a higher temperature between 550 and 650 K Chang [13] measured adsorption isotherms of SO_2 on γ-Al_2O_3 and found a gradual decrease in the amount of SO_2 adsorbed in a temperature region of 298 to 773 K which is in contradiction with the increase of the adsorption parameter b_i between 498 and 525 K as presented in Table 3 Deo and Dalla Lana [10] studied the adsorption of SO_2 on γ-Al_2O_3 using infrared spectroscopy and reported a remarkable change in the infrared absorption spectra between 473 and 573 K The absorption band at 1685 cm^{-1}, observed at temperatures up to 473 K, has disappeared at 573 K and absorption bands at 1440 and 1570 cm^{-1}, that hardly occur up to 473 K, are much stronger at 573 K This indicates that

TABLE 3

Surface diffusion parameters of SO_2 at different temperatures

T (K)	$D_{i,S}^{eff}b_ic_S \times 10^{17}$ $\left(\frac{\text{mole}}{\text{Pa-sec}}\right)$	$b_i \times 10^3$ (Pa^{-1})	$D_{i,S}^{eff}c_S \times 10^{14}$ $\left(\frac{\text{mole}}{\text{sec}}\right)$	Average relative deviation $\sqrt{\frac{CD}{N}}$
447	0 58	−0 01	-	0 033
473	0 65	−0 01	-	0 088
498	0 74	0 11	-	0 022
525	1 50	1 36	1 10	0 062
548	1 31	0 90	1 46	0 058

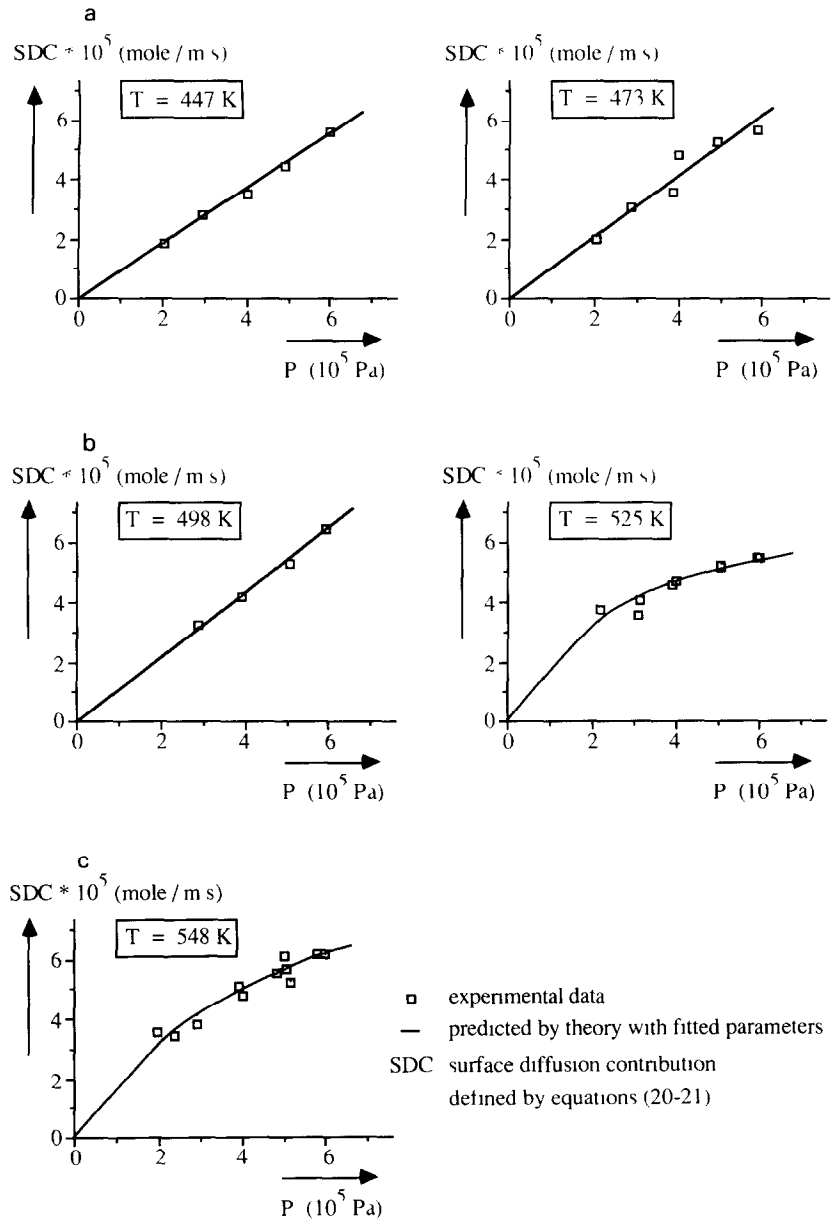

Fig 7 Surface diffusion data of SO_2 as a function of pressure at different temperatures

at 573 K a species is present which was not present at lower temperatures

Although the change in surface diffusion behaviour of SO_2 reported in Table 3 cannot be explained with the results from literature concerning the nature of adsorbed SO_2 it is likely connected to the change in the relative amount of some chemisorbed species.

From the adsorption isotherms measured by Chang [13] the adsorption parameter can be calculated Chang distinguishes two types of adsorbed SO_2, a chemisorbed species and a

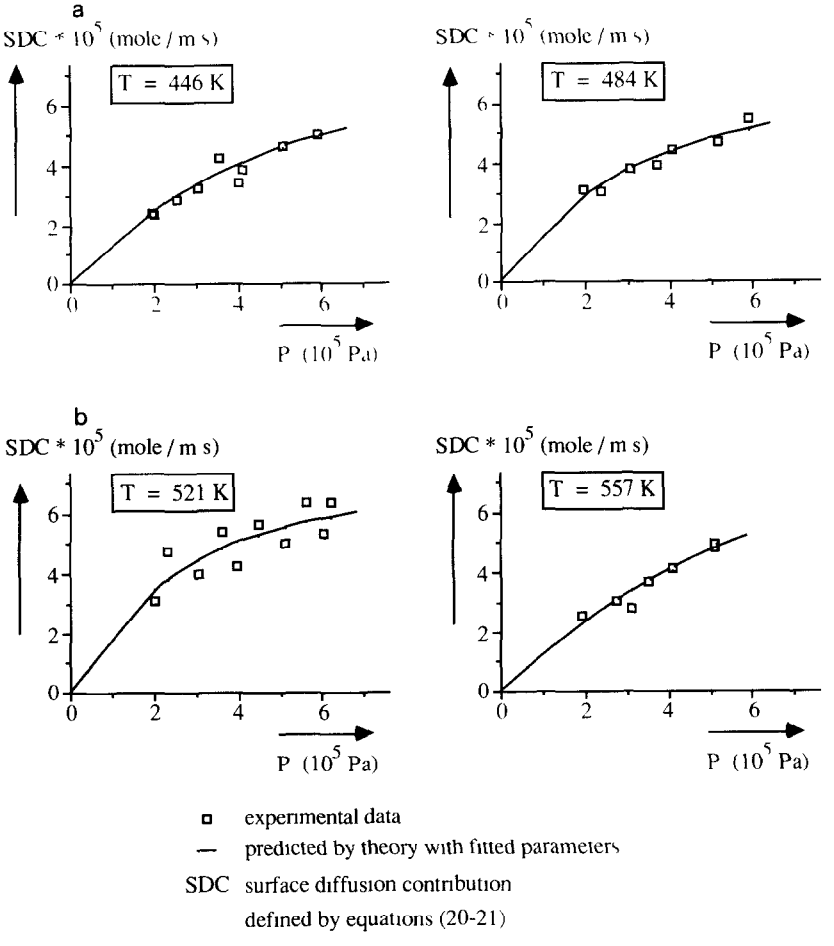

Fig 8 Surface diffusion data of H_2S as a function of pressure at different temperatures

physically adsorbed species. From the total amount of SO_2 adsorbed, consisting of both physically adsorbed and chemisorbed SO_2, an adsorption parameter b_i of 1.1×10^{-3} Pa^{-1} can be calculated from his data at 473 K for a partial pressure of SO_2 of 133 Pa whereas from the amount of physically adsorbed SO_2 only a value of 8×10^{-5} Pa^{-1} can be calculated These values are in reasonable agreement with the data presented in Table 3 and indicate that the chemisorbed species in the present situation is only present at higher temperatures. Gilliland et al [5] reported surface diffusion coefficients of SO_2 in porous glass and porous carbon At a temperature of 288 K they reported values of the surface diffusion coefficient of SO_2 between 5×10^{-9} and 2×10^{-8} m^{-2}-sec^{-1} depending on the heat of adsorption The activation energy of surface diffusion they found was 27 kJ/mole. To calculate the surface diffusion coefficient of SO_2 from the data presented in Table 3, the total concentration of adsorption sites, c_S, is estimated by eqn (23) which is based on monolayer coverage [5]

$$\text{area/molecule} = 1.09\,(m/\rho)^{2/3} \qquad (23)$$

In eqn (23) m is the molar mass and ρ the density of the adsorbate as a saturated liquid

TABLE 4

Surface diffusion parameters of H_2S at different temperatures

T (K)	$D_{i,S}^{eff} b_i c_S \times 10^{17}$ $\left(\frac{\text{mole}}{\text{Pa-sec}}\right)$	$b_i \times 10^3$ (Pa^{-1})	$D_{i,S}^{eff} c_S \times 10^{14}$ $\left(\frac{\text{mole}}{\text{sec}}\right)$	Average relative deviation $\sqrt{\frac{CD}{N}}$
446	0 93	0 75	1 24	0 074
484	1 28	1 25	1 02	0 058
521	1 60	1 00	1 60	0 123
557	0 94	0 51	1 84	0 081

From eqn. (23) a value of c_S of $9\,5 \times 10^{-6}$ mole-m^{-2} is calculated From Table 3 an effective surface diffusion coefficient of SO_2 of about 1×10^{-9} m^{-2}-sec^{-1} results. Using the porosity–tortuosity factor of the membrane of 0 096 a surface diffusion coefficient of SO_2 of 1×10^{-8} m^{-2}-sec^{-1} results which is of the same order of magnitude compared to the values reported in literature by Gilliland et al. [5].

To determine the influence of the mass-transfer parameter in the gas phase outside the membrane, k_g, on the interpretation of the diffusion measurements, eqn. (18), two additional fits were performed One fit uses values for k_g that are increased by 50% and the other fit uses a dependence of k_g of the pressure P of the power $-1/3$ as found in literature [9]. In the last case the constant was adjusted to give the same k_g values at an average pressure of 0.5 MPa. In the first situation, using a 50% higher k_g, the parameters $D_{i,S} b_i c_S$ and b_i fitted were only 4 to 8% lower. Lower values are expected as the decrease of the mass-transfer resistance in the gas phase outside the membrane results in an increase of the driving force over the membrane itself and as a result a larger part of the experimentally observed molar flux is ascribed to diffusion through the gas phase in the pores of the membrane In the second situation, a different pressure dependence of k_g, the surface diffusion parameters fitted deviated less than 1% compared to those presented in Table 3 Therefore the exact relationship giving k_g as a function of pressure is not very important for the interpretation of surface diffusion data in the system used

6 2 *Surface diffusion data of H_2S on γ-Al_2O_3*

Diffusion measurements of H_2S through the membrane as a function of pressure were carried out at temperatures between 446 and 557 K. The contribution of surface diffusion was calculated in the same way as described before. The surface diffusion parameters $D_{i,S} c_S b_i$ and b_i were fitted from the data and the results are presented in Table 4 From Table 4 it seems that both the product $D_{i,S} c_S b_i$ and the adsorption constant b_i show a maximum as a function of temperature whereas the product $D_{i,S} c_S$ increases with temperature A graphical comparison of the experimental data and the theoretical data predicted using the fitted parameters is given in Fig 8

7. Conclusions

It is demonstrated experimentally that surface diffusion of H_2S and SO_2 in an alumina membrane with an average pore diameter of 322 nm, impregnated with γ-Al_2O_3, can contribute substantially to the transport rate Moreover, for this system it is of almost the same order of magnitude as the transport caused by ordinary

diffusion through the gas phase in the pores Owing to the large pore diameter diffusion through the gas phase in the pores of the membrane is determined almost completely by continuum diffusion and the molar flux is therefore independent of pressure. Surface diffusion however is linearly proportional to the pressure provided the fraction of the adsorption sites covered is very low It is demonstrated that the resulting difference in pressure dependence of both transport mechanisms can be used to distinguish between diffusion through the gas phase in the pores and surface diffusion.

As the fraction of the adsorption sites covered with H_2S or SO_2 appears to be considerable, it was necessary to use a two parameter fit, the product $D_{i,S}c_S b_i$ and the adsorption parameter b_i itself, to interpret the surface diffusion data For SO_2 the fitted surface diffusion parameters show a remarkable change between 498 and 525 K which probably can be attributed to the change of some chemisorbed species as has been reported in literature. The order of magnitude of the data found are in reasonable agreement with literature data. For H_2S the parameters fitted show a maximum with temperature, but the product of the effective surface diffusion coefficient and the concentration of adsorption sites increases with temperature.

Acknowledgements

These investigations were supported by the National Dutch Program Comittee on Membranes We also acknowledge K van Bree, W. Leppink and A. Pleiter for the construction of the experimental setup and P Weersink for his part in the experimental work

List of symbols

b_i	adsorption constant (Pa^{-1})
B_0	membrane specific parameter defined in eqn (15) (m^2)
c_S	concentration of adsorption sites (mole-m^{-2})
CD	cumulative relative deviation function between SDC_{exp} and SDC_{theor} (see eqn. 20–22) (–)
d_p	average pore diameter (m)
$D^0_{i,inert}$	continuum diffusion coefficient (m^{-2}-sec^{-1})
$D^0_{i,K}$	Knudsen diffusion coefficient (m^{-2}-sec^{-1})
$D_{i,gas}$	diffusion coefficient in the gas phase in the pores (m^{-2}-sec^{-1})
$D_{i,surf}$	surface diffusion coefficient (m^{-2}-sec^{-1})
$f(d_p)$	volume fraction of the pores with diameter d_p (–)
k_g	mass transfer parameter in the gas phase outside the membrane (m-sec^{-1})
$J_{i,tot}$	total molar flux owing to both transport mechanisms (mole-m^{-2}-sec^{-1})
$J_{i,surf}$	molar flux owing to surface diffusion (mole-m^{-2}-sec^{-1})
L	membrane thickness (m)
M_i	molar mass of component i (kg-$mole^{-1}$)
m	exponent in eqn (17) (–)
n	exponent in eqn (17) (–)
P	pressure (Pa)
R	gas constant (J-$mole^{-1}$-K^{-1})
Re	Reynolds number defined in eqn (17) (–)
Sc	Schmidt number defined in eqn (17) (–)
Sh	Sherwood number defined in eqn. (17) (–)
T	temperature (K)
SDC_{exp}	experimental surface diffusion contribution (see eqn. 20) (mole-m^{-1}-sec^{-1})
SDC_{theor}	theoretical surface diffusion contribution (see eqn 21) (mole-m^{-1}-sec^{-1})

x_i molar fraction of component i (-)
z location inside the membrane (m)

Greek

ϵ porosity of the membrane (-)
η viscosity of the gas (Pa-sec)
ρ density of the gas (kg-m^{-3})
τ tortuosity of the membrane (-)
θ_i fraction of the adsorption sites covered by component i (-)

Subscripts

bulk 0 in the well stirred bulk of the gas at the side of $z=0$
bulk L in the well stirred bulk of the gas at the side of $z=L$
eff effective, corrected for the porosity-tortuosity of the membrane
int 0 at the membrane interface at $z=0$
int L at the membrane interface at $z=L$

References

1 H J Sloot, G F Versteeg and W P M van Swaaij, A non-permselective membrane reactor for chemical processes normally requiring strict stoichiometric feed rates of reactants, Chem Eng Sci , 45 (1990) 2415
2 H F Mark, D F Othmer, C G Overberger and G T Seaborg, Kirk-Othmer, Encyclopedia of Chemical Technology, Vol 22, John Wiley & Sons, New York, NY, 1983, pp 276-282
3 R C Reid, J M Prausnitz and T K Sherwood, The properties of gases and liquids, 3rd edn , McGraw-Hill, New York, NY, 1977
4 R K Smith and A B Metzner, Rates of surface migration of physically adsorbed gases, J Phys Chem , 68 (1964) 2741
5 E R Gilliland, R F Baddour, G P Perkinson and K J Sladek, Diffusion on surfaces I Effect of concentration on the diffusivity of physically adsorbed gases, Ind Eng Chem Fundam , 13 (1974) 95
6 C L Cui, J R Authelin, D Schweich and J Villermaux, Consequence of distributed properties on effective diffusivities in porous solids, Chem Eng Sci , 45 (1990) 2611-2617
7 E A Mason and A P Malinauskas, Gas transport in porous media The dusty-gas model, Chemical Engineering Monographs, Vol 17, Elsevier, Amsterdam, 1983
8 Landolt Bornstein, Zahlenwerte und Funktionen aus Physik, Chemie, Astronomie, Geophysik und Technik, 6e Auflage, II Band, 5e Teil, Bandteil A, 26, Springer Verlag, Berlin, 1969
9 G F Versteeg, P M M Blauwhoff and W P M van Swaaij, The effect of diffusivity on gas-liquid mass transfer in stirred vessels Experiments at atmospheric and elevated pressures, Chem Eng Sci , 42 (1987) 1103
10 A V Deo and I G Dalla Lana, Infrared studies of the adsorption and surface reactions of hydrogen sulfide and sulfur dioxide on some aluminas and zeolites, J Catal , 21 (1971) 270
11 Y Ono, H Takagiwa and S Fukuzumi, Formation of sulfur dioxide anions on alumina, J Catal , 50 (1977) 181
12 H G Karge, S Trevizan de Suarez and I G Dalla Lana, A new cell for combined IR and ESR investigations on solid catalysts, J Phys Chem , 88 (1984) 1782
13 C C Chang, Infrared studies of SO_2 on γ-alumina, J Catal , 53 (1978) 374